CHEMISTRY
A EUROPEAN JOURNAL

DOI: 10.1002/chem.200600760

Polymorphism in Crystalline Cinchomeronic Acid

Dario Braga,[a] Lucia Maini,*[a] Concezio Fagnano,[b] Paola Taddei,*[b] Michele R. Chierotti,*[c] and Roberto Gobetto[c]

Abstract: The structural relationship between the two crystal forms of cinchomeronic acid (**CA** 3,4-dicarboxypyridine) has been investigated by single crystal X-ray diffraction, IR and Raman spectroscopy and solid state NMR spectroscopy, showing that the two polymorphs form a monotropic system, with the orthorhombic form I being the thermodynamically stable form, while the monoclinic form II is unstable. In both forms **CA** crystallizes as a zwitterion and decomposes before melting. The crystal structure and spectroscopic analysis indicate that the difference in stability can be ascribed to the strength of the hydrogen-bonding patterns established by the protonated N-atom and the carboxylic/carboxylate O-atoms.

Keywords: crystal engineering · NMR spectroscopy · polymorphism · pyridinedicarboxylic acid · Raman spectroscopy

Introduction

The phenomenon of polymorphism, namely, the existence of more than one crystal structure for a given compound, is well known and widely studied.[1,2] However, the structural, thermodynamic and kinetic factors associated with the nucleation and crystallization of molecular compounds are not yet fully understood. The experimental investigation of crystal polymorphism is still mainly based on a systematic, and sometimes tedious, exploration of all possible crystallization and interconversion conditions[1–3] ("polymorph screening"), while theoretical polymorph prediction is still embryonic.[4,5] The screening of different crystal forms of a compound is not only an academic challenge but it is becoming one of the most important goals in the pharmaceutical industries, since the majority of drugs are administered as solids and solid-state properties significantly influence the bioavailability and stability of the final product. When two or more polymorphs occur, a full characterisation of these forms and of the relationship among the different solid phases should be studied, which is best achieved by using complementary techniques such as X-ray diffraction, differential scanning calorimetry combined with IR, Raman and solid state NMR (SSMNR) spectroscopy.

Cinchomeronic acid (**CA**, 3,4-dicarboxypyridine) is one of the six isomers of pyridinedicarboxyl acid. All isomers are widely utilized in the construction of coordination networks, since their metal coordination modes allow for different architectures.[6–8] Furthermore some of these isomers are biologically active and **CA** has been studied for its ability to promote the growth of radishes.[9,10] Although **CA** has been known for almost a century[11] and the presence of two forms is reported in the PDF-2[12] since 1971, no scientific report seems to mention the existence of these two polymorphs. The crystal structure of form I (according to the name in PDF-2) was described by Takusagawa et al. in 1973.[13,14]

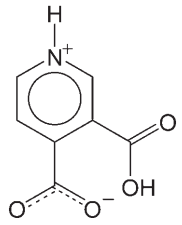

The molecule is present as a zwitterion both in the solid state and in solution,[15] with one acid hydrogen on the ring

[a] Prof. D. Braga, Dr. L. Maini
Dipartimento di Chimica "G. Ciamician"
Università degli studi di Bologna
Via Selmi 2, 40126 Bologna (Italy)
Fax: (+39) 051-209-9456
E-mail: l.maini@unibo.it

[b] Prof. C. Fagnano, Dr. P. Taddei
Dipartimento di Biochimica "Giovanni Moruzzi"
Università degli studi di Bologna
Via Belmeloro, 8/2, 40126 Bologna (Italy)
Fax: (+39) 051-243-119
E-mail: paola.taddei@unibo.it

[c] Dr. M. R. Chierotti, Prof. R. Gobetto
Dipartimento di Chimica I.F.M.
Università di Torino
Via P. Giuria 7, 10125 Torino (Italy)
Fax: (+39) 011-670-7855
E-mail: michele.chierotti@unito.it

nitrogen. The presence of different kinds of acceptor and donor groups for hydrogen bonding makes it a worthy candidate for the study of the competition among of different supramolecular synthons that can be formed.[16]

In this paper the full characterisation by single crystal X-ray diffraction and spectroscopic methods of both form I and II is reported and the preparation of the polymorphs is described. Form II and I were initially obtained as concomitant[17] polymorphs from an ethanol/water solution.

Results and Discussion

Two main reactions are known for the production of **CA**.[18,19] In terms of crystal structures recrystallization of form I (see also Experimental Section) from EtOH, MeOH, EtOH/H_2O, MeOH/H_2O yields form I or a mixture of form I with a small portion of form II. Form I and II appeared concomitantly as rods (form I) and blocks (form II) as shown in Figure 1 from recrystallization of form II in ethanol/water solution. Form II was produced quantitatively by acidification with HCl (pH≈2) of a water solution of Na-[$C_7H_4NO_4$]. Conversion of form II to form I was observed via slurry conversion experiment. The two polymorphs decompose before melting.[20] The decomposition temperature was measured several times with capillary methods revealing that form II decomposes always at lower temperature than form I: with a scan speed of 2 °C min^{-1} **CA** form I decomposed at 263 °C while form II decomposed at 259 °C. Since in DSC no interconversion between the two compounds is present, we surmise that a monotropic system is present where form I is the thermodynamic stable phase, while form II is the metastable one.[21]

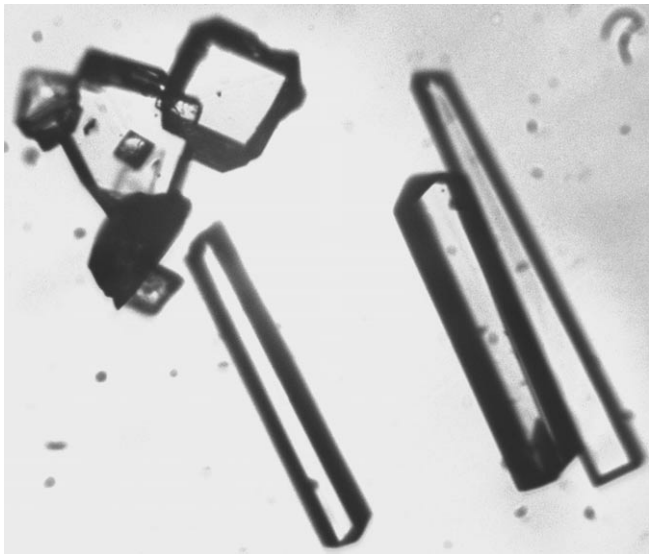

Figure 1. Concomitant polymorphs obtained from a ethanol/water solution, rods: form I, blocks: form II.

Crystal structure of form I: The form I of 3,4-pyridinedicarboxylic acid crystallizes with a rod-like habit in the orthorhombic system, for which we have re-determined the crystal structure previously reported by Takusagawa.[13] Although no significant differences were found, our crystal structure is used for the discussion in preference to the one previously reported because of a slightly better structural model. The internal geometry of **CA** conforms to the zwitterionic form of the other pyridinedicarboxylic isomers (2,3-pyridinedicarboxylic[22] and 3,5-pyridinedicarboxylic[23,24]). The carboxylic group [$C_6(=O_2)$-O_1-H_{101}] is tilted with respect to the aromatic ring with a torsional angle of −40.8° [C_1-C_2-C_6-O_1]. The C−O bond lengths of C_6=O_2 1.213(2) Å and C_6−O_1 1.301(2) Å are in agreement with the average values tabulated by Allen[25] in which C=O distance is 1.23(2) and C−O is 1.31(2) Å for a carboxylic group attached to an aromatic ring (see Figure 2). This carboxylic acid donates the hydrogen to the neighbouring carboxylate forming a hydrogen bond,[26] and its carbonyl group is involved in a quite short C-H···O interaction (C-H···O 2.27 Å with C–H distance normalized to 1.08 Å, see Table 1). The carboxylate group forms a torsion angle of −73.9° [C_2-C_3-C_7-O_3] with the aromatic ring; as shown in the Figure 2 the two groups are rotated in the same direction. The C−O distances in the carboxylate group, C_7–O_3 1.253(2) and C_7–O_4 1.233(2), are similar and correspond to the C–O lengths in carboxylate moieties reported by Allen (1.26(1) Å). The C_1-N_1-C_6 angle of 122.4° corresponds to the average C-N-C angle in pyridinium ions 122.0(2)°.[27]

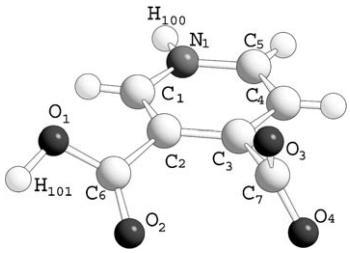

Figure 2. Structure of CA in form I together with the labelling scheme.

Table 1. Hydrogen bonds in form I.

D-H···A	D−H [Å]	H···A [Å]	D···A [Å]	D-H···A [°]
O1-H101···O3	1.02(2)	1.49(2)	2.5068(14)	173(2)
N1-H100···O4	0.92(2)	1.79(2)	2.6636(15)	156.9(19)
C1-H1···O1	1.08	2.47	3.2971	133
C5-H5···O2	1.08	2.27	3.2887	156

The crystal structure consists of chains of the acid molecules interacting via short hydrogen bonds between the carboxylic and the carboxylate groups (2.5068(14) Å). Each 3,4-pyridinedicarboxylic acid molecule forms four hydrogen bonds in a sort of tetrahedral coordination arrangement to give a three-dimensional adamantoid network. The large

cavity present within each adamantoid cage is filled by interpenetration of two other, symmetry-related, adamantoid networks, giving a total of three interpenetrating networks (see Figure 3).

Crystal structure of form II: Form II of 3,4-pyridinedicarboxylic acid crystallises with a block-like habit in the monoclinic system. The asymmetric unit consists of half a molecule, the whole molecule is generated by the two-fold axis lying in the plane of the aromatic ring between the two functional groups. Since the molecule does not possess this symmetry operation, the crystal symmetry results in a disordered positioning of the C_3 and N_1 atoms with site occupancy 50:50. This particular situation generates two crystallographically equivalent, space-averaged, -COO(-COOH) groups. The C_4–O_1 and C_4–O_2 (see Figure 4) distances of 1.208(4) and 1.273(4) Å, respectively, correspond to the average of the distances of C–O and C=O of the carboxylic and carboxylate groups. However the short C_4–O_1 distances of 1.208(4) suggests that the C–O bond lengths in the carboxylate group are not equal, due to the presence of the strong hydrogen bond (O_2–O_2 2.472(5) Å), which is also supported by the IR, Raman and solid state NMR data (see below). The hydrogen atoms were not observed in the Fourier map and the zwitterionic nature of **CA** in form II was inferred from the hydrogen-bonding pattern, the geometry parameters and spectroscopic evidence. The C_2-N_1-C_3 angle of 124.4° is closer to the average C-N-C angle in pyridinium ions 122.0(2)° than in pyridyl molecules (117.3(2)°) and the protonation of the nitrogen is consistent to IR, Raman and SSNMR

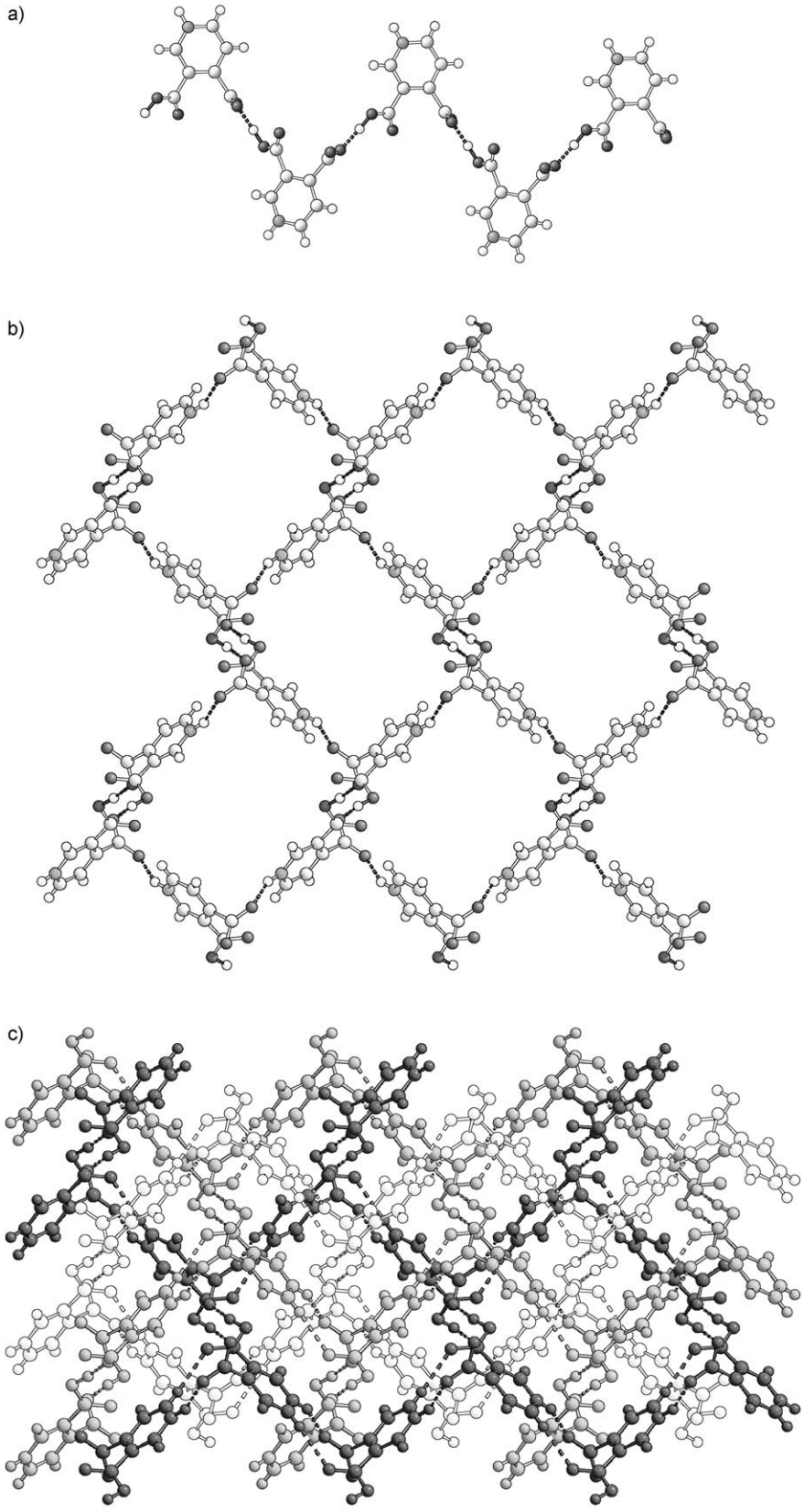

Figure 3. Chains present in form I (a); the adamantoid network formed by N-H^+···O^- hydrogen bonds among the chains (b) and the overall crystal structure formed by the three interpenetrating networks (c).

measurements. The carboxylic and carboxylate groups are tilted with respect to the aromatic ring with an average torsion angle of −55.1°.

As well in form I, in **CA** form II the short hydrogen bond between the carboxylic and carboxylate groups (O_2–O_2 2.472(5) Å; Table 2) generates infinitive chains, and these run parallel to each other and the groove of one chain is filled by the hunches of the adjacent chains (Figure 5). This structure brings the oxygen atom not involved in the short hydrogen bond close to the nitrogen atom and to the crystallographically equivalent carbon (2.958(5) Å). The apparent lengthening of the N-H^+···O^- interaction compared with the hydrogen bond present in form I as well as and the short C-H···O interaction is a consequence of this disorder inside the crystal structure. The chains run parallel to each other and are linked by the N-H^+···O^- hydrogen bonds forming a two dimensional network. The resulting layers are laid one on the top of the other.

It is worth noting that both polymorphs prefer the formation of intermolecular O-H···O interactions over that of the intramolecular hydrogen bonds, although the molecular geometry makes intra-molecular bonding possible as observed in the structure of 2,3-pyridinedicarboxylic acid. Moreover, ab initio calculations on the hydrogen-bond strength of **CA** suggest that the intramolecular bond in gas phase is more stable than the intermolecular one.[15] However, all the experimental evidence confirms the presence of the intermolecular hydrogen bond between the carboxylic and carboxylate groups. While in the kinetic form II the chains are disordered and the entropic factors are maximized, during crystallization of form I, the stable one, the molecules had time to order up and optimize the formation of hydrogen bonds to decrease the lattice energy.

IR and Raman measurements: Figures 6 and 7 show the IR and Raman spectra of the two polymorphs of **CA**. As far as

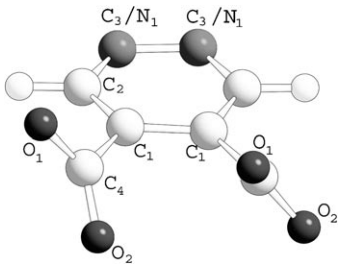

Figure 4. Structure of **CA** in crystals of form II; the atom C3 and N1 are disordered with occupancy 50:50 over the same position.

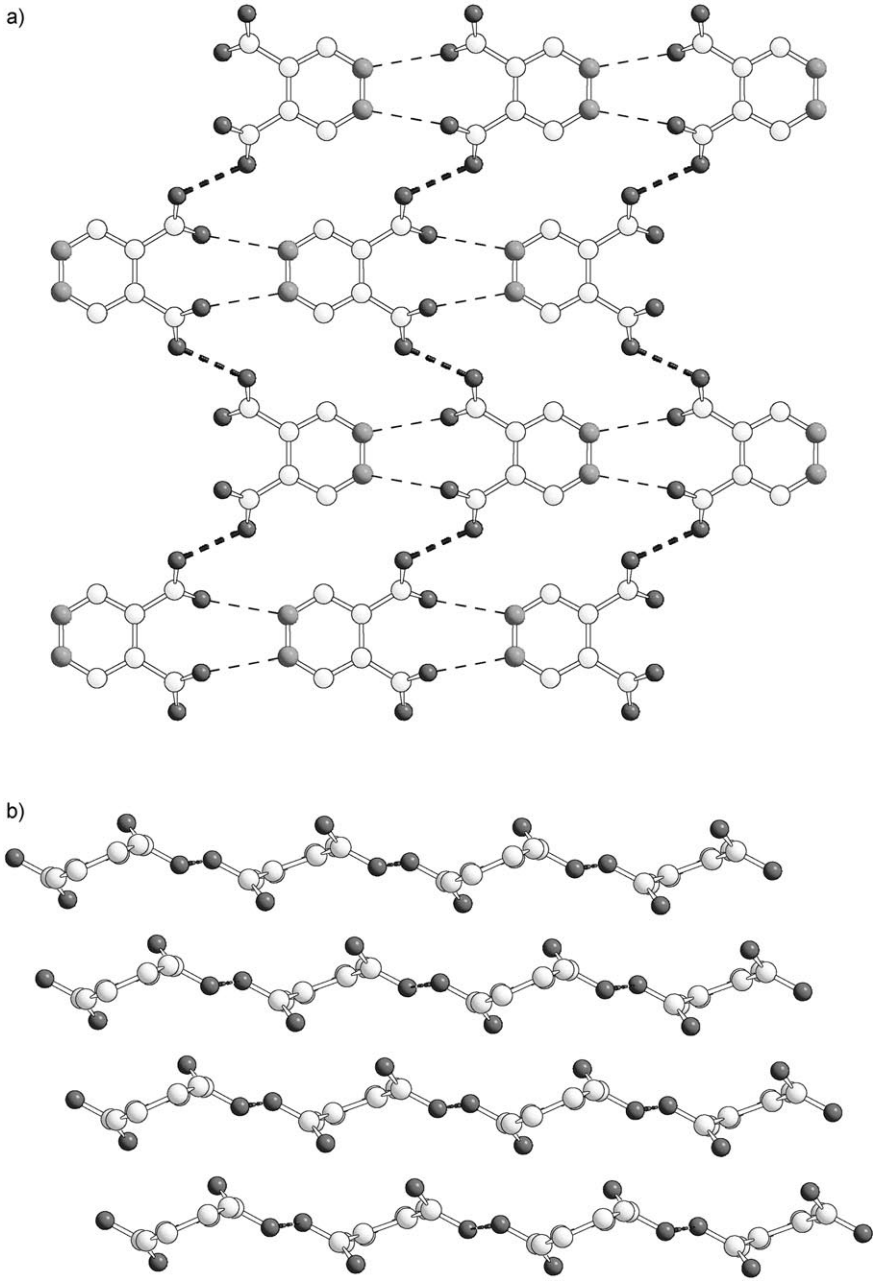

Figure 5. Hydrogen bonded chains formed by molecules of **CA** in form II and the interactions N-H^+···O^- and C-H···O^- among the chains a); and the crystal structure view along the *b* axis b).

Table 2. Hydrogen bonds in form II.

D-H···A	D···A [Å]
O2−O2	2.472(5)
N1−O1	2.957(5)
C3−O1	2.957(5)

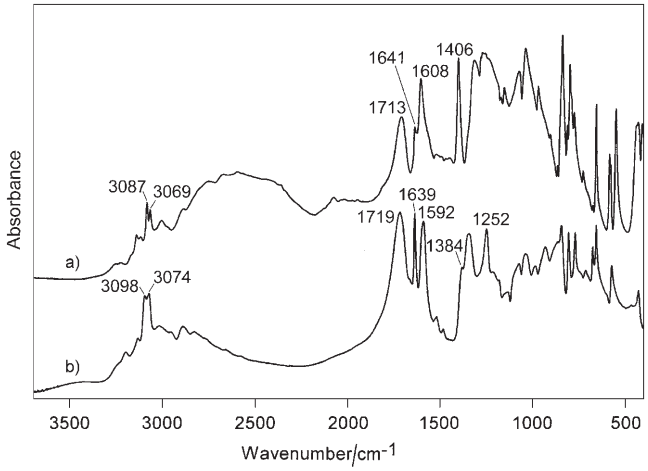

Figure 6. IR spectra of the two polymorphs of **CA**: a) form I; b) form II.

we know, IR and Raman spectroscopies have been used here for the first time to distinguish the two polymorphic forms of **CA**. Wasylina et al.[28] and Harmon and Shaw[15] have reported the IR spectrum of only one polymorphic form of **CA** and have given partial vibrational assignments. Several metal complexes of **CA** have been characterised by IR[7,29–32] and Raman[33] spectroscopies.

As can be easily seen from Figures 6 and 7, the two polymorphs show significant differences in both IR and Raman spectra for either the presence of some bands only for one polymorph or the wavenumber positions of many bands or their relative intensities.

The IR spectrum of form I (Figure 6a) shows a broad absorption in the $\tilde{\nu}=3300$–$2300\ cm^{-1}$ region, centred at about $2600\ cm^{-1}$. Also the IR spectrum of the form II (Figure 6b) shows an analogous broadening, but its maximum appears shifted to higher wavenumbers (i.e., about $2900\ cm^{-1}$). Both spectral features can be ascribed to νNH stretching modes of hydrogen-bonded NH groups.[29]

A reasonably good correlation between νOH stretching frequencies and d(O···O) distances in O-H···O hydrogen-bonded systems has been proposed.[34] According to this correlation, the frequency shifts to lower wavenumbers with shortening of the hydrogen bond. Although N-H···O hydrogen-bonded systems have been investigated less extensively than O-H···O ones, a similar correlation can be considered valid. Thus, it can be affirmed that N-H···O hydrogen bonds are shorter in form I than in form II. This result is in agreement with the diffraction data which indicated the presence of stronger N-H···O hydrogen bonds in the form I (2.6636(15) Å) than in the form II (2.957(5) Å).

The IR spectra of the two polymorphs show also broad, strong structured absorptions in the 1400–400 cm^{-1} range, which are characteristic of strong three-centre O-H-O hydrogen bonds.[34] The spectral pattern is similar to that observed in several acid salts of carboxylic acids:[34] the νOH band has been reported to appear as a very broad absorption extending over several hundreds cm^{-1} interrupted by Evans-type transmission "windows". In the IR spectra of the two polymorphs of **CA** (Figure 6), the centre of these absorptions appears at different wavenumber positions, revealing the presence of hydrogen bonds of different strengths. More in details, for form II the centre appears shifted to lower wavenumber values than for form I. Such shift suggests the presence of a stronger O-H-O interaction in II, which is consistent with the hydrogen bond distances observed in the structures.

Similar broadening was not observed in the Raman spectra of the two polymorphs (Figure 7). Actually, Raman spectroscopy has proved less sensitive to hydrogen-bonding arrangements.[34,35]

Other spectral features can be related to the different bond lengths and hydrogen-bonding systems present in the two polymorphs. Concerning the carboxylic group, its main vibrational features are the νC=O and νC−O stretching modes. The latter can correspond to the IR band at about $1250\ cm^{-1}$[28] which appears quite sharp in the spectrum of form II (Figure 6b) whereas the band is broader in form I (Figure 6a). In the Raman spectra (Figure 7), a band at a similar wavenumber position was observed (at $1254\ cm^{-1}$ for form I and

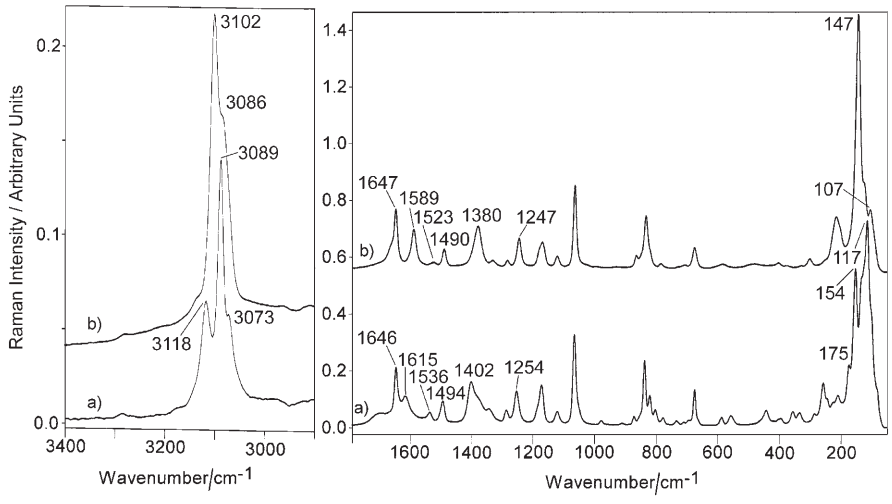

Figure 7. Raman spectra of the two polymorphs of cinchomeronic acid: a) form I; b) form II.

1247 cm^{-1} for form II). The νC=O stretching mode of the carboxylic group appears as a strong band in both IR spectra of Figure 6. This mode falls at $\tilde{\nu}=1713$ and at 1719 cm^{-1}, respectively, for form I and form II, that is, at wavenumber positions similar to that of pyridine carboxylic acids.[36] The relative wavenumber position of this mode in the two polymorphs suggests that in form II the C=O bond should be stronger. In the Raman spectra (Figure 7), the νC=O mode is noticeably weaker and more difficult to be localised, as previously observed for similar systems;[37] a broad Raman band at about 1700 cm^{-1} was observed only for form I (Figure 7a).

Concerning the carboxylate group, it must be recalled that when a carboxylate salt is made from a carboxylic acid, the C=O and C–O bonds are replaced by two equivalent carbon–oxygen bonds which are intermediate in force constant between the C=O and C–O. These two oscillators are strongly coupled resulting in an asymmetric COO^- stretching vibration ($\nu_{as}COO^-$) at 1650–1540 cm^{-1} and a symmetric COO^- stretching vibration (ν_sCOO^-) at 1450–1360 cm^{-1}.[38] In case of multiple unsymmetrical hydrogen bonds to COO^- groups, one CO will have a little more single bond character and the other a little more double bond character. This leads to higher differences between the $\nu_{as}COO^-$ and ν_sCOO^- values ($\Delta\nu=\nu_{as}COO^- - \nu_sCOO^-$) than in the case of two equal CO bonds. The same is true when a metal is more strongly associated with one oxygen of the COO^- group than the other: $\Delta\nu$ is higher than in the case of sodium salts, where the CO bonds are equal.[39]

The assignment of the $\nu_{as}COO^-$ and ν_sCOO^- modes in the spectra of the polymorphs of **CA** can be a challenging task; actually, the 1650–1350 cm^{-1} range is a complex spectral region since it contains the bands which result from the stretching vibrations of the heterocyclic ring (νCC, νCN) and of the carboxylate group ($\nu_{as}COO^-$ and ν_sCOO^-). In the case of form I, the IR $\nu_{as}COO^-$ and ν_sCOO^- modes appear at 1641 and 1406 cm^{-1}, respectively (Figure 6a). Similar wavenumber values have been reported for these modes in dibutyltin(IV) complexes of **CA**.[29] In the Raman spectrum of form I (Figure 7a), the corresponding bands were observed at similar wavenumber positions (1646 and 1402 cm^{-1}). In form II, the $\nu_{as}COO^-$ mode falls nearly in the same wavenumber position as in form I (1639 and 1647 cm^{-1} in the IR and Raman spectra, respectively, Figures 6b and 7b), while the ν_sCOO^- mode shifts to lower wavenumber values (1384 and 1380 cm^{-1} in the IR and Raman spectra, respectively, Figures 6b and 7b). Therefore, in form II the $\Delta\nu$ difference between the $\nu_{as}COO^-$ and ν_sCOO^- modes appears higher than in form I. This result is consistent with the other information: in form I the carboxylate group shows almost equal C–O distances and both oxygen atoms are involved in hydrogen bonds (with the carboxylic acid and the pyridinium), in form II the X-ray data are less helpful since the CO distances are averaged values between the carboxylic and carboxylate group. However the ^{13}C SSNMR indicates the presence of a carboxylate group with an intermediate character between a carboxylic and carboxylate, inasmuch as the C=O and C–O bond lengths appeared more differentiated than in form I (see below).

The IR band at 1608 cm^{-1} in the spectrum of form I (Figure 6a) can be attributed to the skeleton vibration of the pyridine ring[28,37] as well as the corresponding Raman band at 1615 cm^{-1} (Figure 7a). In the spectra of form II, this vibrational mode appears shifted to lower wavenumbers (1592 and 1589 cm^{-1} in the IR and Raman spectra, respectively, Figures 6b and 7b). A detectable shift involves also the IR bands due to the aromatic C–H stretching vibrations: in the spectra of form I and II they appear at $\tilde{\nu}=3087$–3069 and 3098–3074 cm^{-1}, respectively. In the corresponding Raman range, form I shows three bands at 3118, 3089 and 3073 cm^{-1} (Figure 7a), while form II is characterised by a prominent band at 3102 cm^{-1} with a shoulder at 3086 cm^{-1} (Figure 7b). These different spectral patterns can arise as a result of overtones from other vibrational modes or from crystal splitting effects. However, for this purpose, it must be stressed that the Raman spectrum of form II shows a minor number of distinct components than that of form I (two instead of three). The same behaviour is clearly observable also in the spectral range below 1000 cm^{-1} (Figure 7) and can be related to the disorder inside the crystal structure of form II.

The Raman spectral region below 200 cm^{-1} has proved to be a valid tool for the recognition of different polymorphic forms,[35] since lattice vibrations fall in this range. As can be easily seen from Figure 7, the two polymorphs of **CA** show significant differences in both the wavenumber positions and relative intensities of the low frequency bands, clearly reflecting the existence of two different crystalline unit cells characteristic of the two polymorphic forms.

SSNMR measurements: All NMR data are reported in Table 3. The ^{13}C CPMAS spectrum of form I (Figure 8a) shows two resonances in the carboxylic region at δ 172.0 and at 167.5 ppm, respectively, in agreement with the presence of two different groups observed in the X-ray structure. The former is attributed to the COO^- group with C–O distances of 1.2526(16) and 1.2331(15) Å, while the latter to the COOH group with C–O distances of 1.3005(15) and 1.2126(16) Å. Other parameters for determining the carboxylic or carboxylate character are the chemical shift tensors, listed in Table 3, obtained by spinning sideband analysis[40] As previously reported,[41] the carboxylate group is characterized by higher δ_{22} ((159.7 ppm) and lower δ_{11} (160.3 ppm) values with respect to the carboxylic group (($\delta_{22}=138.7$ ppm and $\delta_{11}=264.6$ ppm). The δ_{33} tensor is not very sensitive to the protonation state. The difference of 21 ppm between the two δ_{22} values confirms the reliability of these data.

The carboxylate group is involved in two hydrogen-bond interactions, one with the pyridine nitrogen and the other with a COOH group. In the former the presence of a proper base yields a proton transfer from the acid to the nitrogen (Table 3). The proton involved in the O···H-N interaction falls at δ 15.1 ppm in the ^1H MAS spectrum (Figure 9a), characteristic of a weak-intermediate interaction, as con-

Table 3. Chemical shift for form I and form II.

Compound	^{1}H [ppm]	^{15}N [ppm]	^{13}C [ppm]	δ_{11}	δ_{22}	δ_{33}
form I	16.2	179.5	172.0* (COO^-)	260.3	159.7	96.6
	15.1		167.5* (COOH)	264.6	138.7	99.6
	8.4		155.0* (C4)			
	7.5		144.8 (C2-C6)			
	6.6		128.9* (C3)			
			124.8 (C5)			
form II	18.1	176.1	170.6* (COOH/COO^-)	274.2	150.7	87.5
	13.0		151.9* (C4)			
	7.7		146.5 (C2)			
			143.5 (C6)			
			130.8* (C3)			
			126.1 (C5)			

[*] C quaternary.

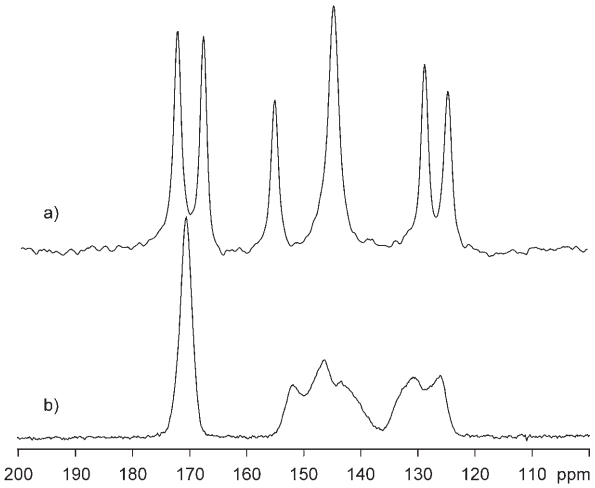

Figure 8. ^{13}C CPMAS spectra of **CA**: a) form I and b) form II recorded at 67.9 MHz with a spinning speed of 5 kHz.

firmed also by the large distance from the heavy atom (2.6636(15) Å). Conversely, the carboxylic group does not yield the proton transfer reaction and it forms a strong-intermediate interaction O-H···O characterized by a short heavy atom distance (2.5068(14) Å) and by a proton chemical shift of 16.2 ppm (Figure 9a). In the ^{1}H MAS spectrum the three

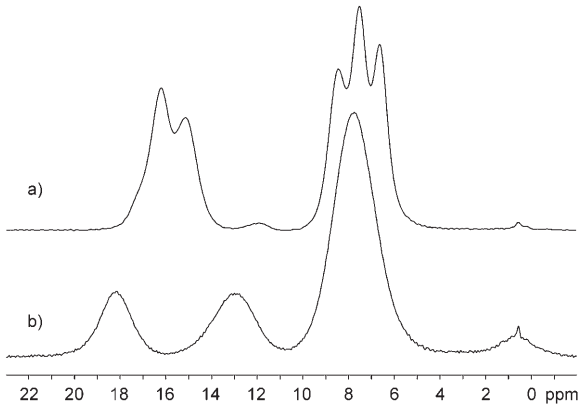

Figure 9. ^{1}H MAS spectra of **CA**: a) form I and b) form II recorded at 600 MHz with a spinning speed of 35 kHz.

peaks in the aromatic region at 8.4, 7.5 and 6.6 ppm have been assigned to H_2, H_6, and H_5 protons, respectively.

The protonation of the pyridine nitrogen is also confirmed by the ^{15}N CPMAS spectrum (Figure 10) that shows a single resonance at δ 179.5 ppm. Indeed, the free pyridine nitrogen signal falls at 293.8 ppm and it is well known that the presence of a hydrogen bond on aromatic amines leads to a low-frequency shift.[42] In this case the shift observed is quite large (114.3 ppm), probably due to the concomitant presence of COOH groups in *meta*- and *para*-positions.

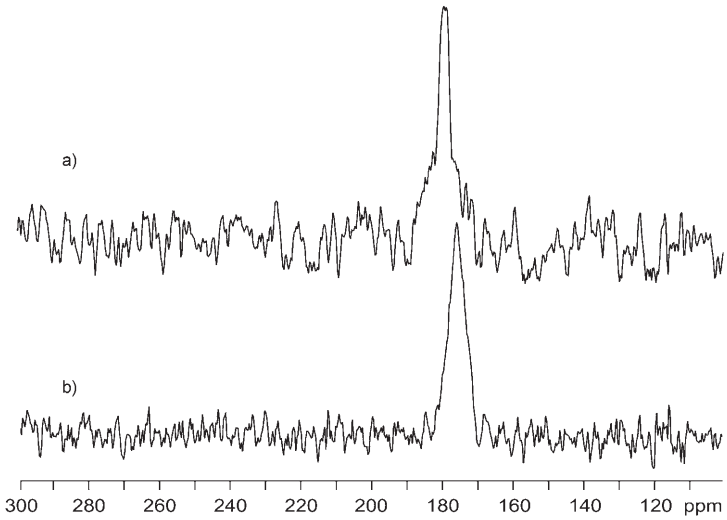

Figure 10. ^{15}N CPMAS spectra of cinchomeronic acid: a) form I and b) form II recorded at 27.2 MHz with a spinning speed of 5 kHz.

A single resonance located at 170.6 ppm is present in the carboxylic region of the ^{13}C CPMAS spectrum of form II (Figure 8b). This chemical shift value is indicative of an intermediate situation between a carboxylic and carboxylate character, in complete agreement with the presence of two equal COOH groups with C–O distances of 1.208(4) and 1.273(4) Å observed in the X-ray structure. The linewidth (166 Hz) is twice as wide with respect to the peaks (COOH 80 Hz and COO^- 80 Hz) of form I in agreement with the presence of a static disorder detected by X-ray. The disorder is also confirmed by the broad and partially overlapped pyridine carbon resonances in the ^{13}C spectrum. Thus, in this case, X-ray and SSNMR give an average value of the COOH group, while IR and Raman data are able to distinguish between two slightly different groups: one with a more carboxylic character and the other with a pronounced carboxylate character. Again the δ_{22} value (Table 3), as the isotropic chemical shift, is intermediate (150.7 ppm) between the carboxylic and carboxylate δ_{22} values observed for form I.

The COOH group is involved in both an O···H-N and a O···H-O hydrogen bonds. In the former the proton is transferred from the acid to the base as confirmed by the ^{15}N CPMAS resonance at 176.1 ppm (Figure 10b). In this case the nitrogen signal is more displaced that in form I probably because the nitrogen lone pair is partially removed due to a

closer proton position and to the larger heavy atom distance (2.957(5) Å). The larger O–N distance and the low frequency hydrogen bonded proton peak at 13.0 ppm in the ^{1}H MAS spectrum (Figure 9b) enable us to classify it as a weak interaction. Conversely the O···H-O is a strong interaction as confirmed by the short O–O distance (2.472(5) Å) and by the hydrogen-bonded proton signal at 18.1 ppm.

Conclusion

In this paper we reported the results of an investigation of the crystal polymorphism of **CA**. In order to fully understand the relationship between the two crystal phases of this widely used molecule a comparative use of diffraction and solid state spectroscopy has been exploited. The form I and II of **CA** constitute a monotropic system, that is, the two crystals do not interconvert at any given temperature before melting or decomposition. The form I is the thermodynamically stable form and decomposes at 263 °C, while the latter is the metastable form and decomposes at 259 °C. The single crystal structures give us a view of the hydrogen bonds formed by the molecule of **CA** in the solid state while the zwitterionic nature is confirmed by the spectroscopic measurements. In both structures the molecules of **CA** form infinite chains via short O-H···O hydrogen bonds between the carboxylic and carboxylate groups. The intermolecular chain appears to be favoured over the alternative possibility offered by the intramolecular hydrogen bond. In form I the zwitterion chains are ordered and are connected via N-H···O interactions to form a three-fold interpenetrating networks. In form II, on the other hand, the presence of static disorder leads to crystallographic equivalence between the -COO and -COOH groups. The SSNMR spectrum of form II also shows a chemical shift indicative of an intermediate situation between a carboxylic and carboxylate character. The presence of a carboxylate group with unequal C–O bond lengths is also consistent with the IR and Raman spectra.

The solid state NMR, IR and Raman spectra confirm the presence of strong N-H···O interactions in form I while in form II they are significantly weaker. The possibility of optimizing the hydrogen bond interaction in form I, with respect to the somewhat *looser* interactions allowed by the packing in form II might be responsible for the stabilization of the crystal structure of form I.

On closing, this study demonstrates how the use of different and complementary techniques affords a thorough understanding of the nature and structural relationship of crystal polymorphs.

Experimental Section

CA was purchased twice form Aldrich and used without further purification. The first batch was characterized as pure form II from the powder diffraction database (PDF-2 by ICDD) and recrystallization from ethanol/water solution yielded rod (form I) and block (form II) crystals suitable for X-ray single crystal. The second batch purchased was characterized as the pure form I reported by Takusagawa,[13] and recrystallization from ethanol, methanol, water and mixture of them yielded crystal or crystalline powder of form I and in some cases with a small portion of form II. Form II can also be obtained quantitatively by precipitation of the water-soluble sodium salt of **CA** with HCl. It may well be that the two batches came from a different production, since two main reactions are known for the production of **CA**.[18,19]

Crystallization of form II: A sample of **CA** form I (300 mg) was dissolved in NaOH (18 mL, 0.1 M). The solution was concentrated on a rotary evaporator to obtain a white solid. The $Na(C_7H_4O_4N)$ was dissolved in the minimum amount of water and HCL concentrated was added dropwise until the formation of a precipitate. The solid (**CA** form II) was filtered and washed with methanol and characterized by X-ray powder diffraction.

Slurry experiment: A sample of **CA** form II (100 mg) was suspended in methanol (0.5 mL) and stirred in a closed vessel in presence of seeds of form I for one week. X-ray powder diffraction confirmed the complete conversion of form II to I.

Raman spectroscopy: Raman spectra were recorded on a Bruker IFS66 spectrometer equipped with a FRA-106 FT-Raman module and a cooled Ge-diode detector. The excitation source was a Nd^{3+}/YAG laser (1064 nm) in the backscattering (180°) configuration. The focused laser beam diameter was about 100 μm, the spectral resolution was 4 cm^{-1}, and the laser power at the sample was about 50 mW.

Melting point apparatus: The melting point was observed with a Buchi B-540 at rate 2 K min^{-1}.

IR spectroscopy: IR spectra were measured on a Nicolet 5700 Fourier Transform spectrophotometer (Thermo Electron Corporation) using KBr pellets (about 0.5 % w/w). The spectral resolution was 4 cm^{-1}.

NMR spectroscopy: All ^{13}C and ^{15}N NMR spectra were obtained by using a Jeol GSE 270 (6.34 T) spectrometer operating at 67.9 MHz for ^{13}C and at 27.25 MHz for ^{15}N, equipped with a Doty XC5 probe. The spectra were recorded at a spinning rate in the range from 5–6 kHz under conditions of ^{1}H,^{13}C cross-polarization, high power proton decoupling and magic angle spinning. The 90° pulse was 4.5 μs and the contact pulse was 3.5 ms. The spectra were collected after 1500 scans using a recycle delay of 10 s. The line broadening was set to be 10 Hz. The ^{15}N CPMAS spectra were recorded at a spinning rate of about 5 kHz. A contact time of 5 ms, a repetition time of 10 s, and a spectral width of 35 kHz were used for accumulation of 3600 transients. The fids were processed with a line broadening of 25 Hz. Cylindrical 5 mm o.d. zirconium rotors with sample volume of 120 μL were employed. For all samples the magic angle was carefully adjusted from the ^{79}Br MAS spectrum of KBr by minimizing the line width of the spinning side band satellite transitions. The ^{13}C Chemical shifts were referred to external hexamethylbenzene, setting the methyl carbon to 17.4 ppm downfield from tetramethylsilane (TMS), while the ^{15}N chemical shifts were referenced via the resonance of solid $(NH_4)_2SO_4$ (−355.8 ppm with respect to CH_3NO_2).

The principal components of the chemical shift tensors were extracted by computer simulation (HBA-graphical)[43] of the spinning sideband patterns obtained at low speed using the algorithm developed by Herzfeld and Berger.[40] The errors in the evaluation of the chemical shift tensor were estimated to be less than 4 ppm by repeating the calculation at different spinning speeds. The chemical shift tensors were reported following the standard convention where $\delta_{11} > \delta_{22} > \delta_{33}$, $\delta_{iso} = (\delta_{11}+\delta_{22}+\delta_{33})/3$ and $\Delta\delta = \delta_{33} - (\delta_{11}+\delta_{22})/2$.

^{1}H MAS spectra were recorded on a Bruker AVANCE600WB spectrometer operating at 600 MHz for ^{1}H. Powdered samples were spun at about 30–35 kHz in a 2.5 mm MAS BB probe. Spectra were acquired using an airing sequence for minimizing the proton background signal of the probe with a $\pi/2$ pulse duration of 2.5 μs and a pulse delay of 10 s over a spectral width of 100 kHz. A total of 16 transients were collected for each spectrum. Proton chemical shifts were referenced via the resonance of PDMSO (poly-dimethylsiloxane) at 0.14 ppm relative to TMS.

X-ray crystallography: X-ray diffraction data of **CA** form I was measured on a Apex II Bruxer AXS diffractometer and that of form II was measured on a NONIUS CAD-4 diffractometer. Common to both compounds: $Mo_{K\alpha}$ radiation, $\lambda = 0.71073$ Å, monochromator graphite. Crystal data and details of measurements are reported in Table 4. SHELXS97 and SHELXL97 were used for structure solution and refinement based on F^2.[44] SCHAKAL99 was used for the graphical representation of the results.[45]

CCDC-609435–609436 contain the supplementary crystallographic data for this paper. These data can be obtained free of charge from The Cambridge Crystallographic Data Centre via www.ccdc.cam.ac.uk/data_request/cif.

Table 4. Crystal data and details of measurements for **CA** form I and II.

	Form I	Form II
formula	$C_7H_5NO_4$	$C_7H_5NO_4$
M_w	167.12	167.12
T [K]	293(2)	293(2)
system	orthorhombic	monoclinic
space group	$P2_12_12_1$	$C2/$
a [Å]	5.2864(4)	7.665(2
b [Å]	11.1966(8)	7.305(2)
c [Å]	11.2293(8)	12.148(3)
β [°]	90°	104.57(2)°
V [Å^3]	664.66(8)	658.3(3)
Z	4	4
$F(000)$	344	344
θ range	3–28	3–25
$\mu(Mo_{K\alpha})$ [mm^{-1}]	0.140	0.142
measured reflns	7790	612
unique reflns	1584	582
refined parameters	118	56
GOF on F^2	1.056	1.048
$R1$(onF, $I > 2\sigma(I)$)	0.0271	0.0525
$wR2$ (F^2, all data)	0.0737	0.1675

Acknowledgements

D.B. thanks Marco Serra for the crystallization of the acid and Dott. K. Rubini for the DSC measurements. We thank Hans Foester (Bruker Biospin, Karlsruhe, Germany) for recording the 600 MHz proton measurements.

[1] J. Bernstein, *Polymorphism in Molecular Crystals*, Oxford University Press, Oxford, **2002**, p. 352.
[2] H. G. Brittain, *Polymorphism in Pharmaceutical Solids*, Marcel Dekker, Inc, New York, **1999**, p. 427.
[3] R. Hilfiker, *Polymorphism*, Wiley-VCH, Weinheim, **2006**.
[4] G. M. Day, W. D. S. Motherwell, H. L. Ammon, S. X. M. Boerrigter, R. G. Della Valle, E. Venuti, A. Dzyabchenko, J. D. Dunitz, B. Schweizer, B. P. van Eijck, P. Erk, J. C. Facelli, V. E. Bazterra, M. B. Ferraro, D. W. M. Hofmann, F. J. J. Leusen, C. Liang, C. C. Pantelides, P. G. Karamertzanis, S. L. Price, T. C. Lewis, H. Nowell, A. Torrisi, H. A. Scheraga, Y. A. Arnautova, M. U. Schmidt, P. Verwer, *Acta Crystallogr. Sect. B Struct. Sci.* **2005**, *61*, 511–527.
[5] S. Datta, D. J. W. Grant, *Nat. Rev. Drug Discovery* **2004**, *3*, 42–57.
[6] M. L. Tong, J. Wang, S. Hu, S. R. Batten, *Inorg. Chem. Commun.* **2005**, *8*, 48–51.
[7] M. L. Tong, J. Wang, S. Hu, *J. Solid State Chem.* **2005**, *178*, 1518–1525.
[8] M. K. I. Senevirathna, P. Pitigala, V. P. S. Perera, K. Tennakone, *Langmuir* **2005**, *21*, 2997–3001.
[9] H. Nishitani, K. Nishitsuji, K. Okumura, H. Taguchi, *Phytochemistry* **1996**, *42*, 1–6.
[10] H. Taguchi, M. Maeda, H. Nishitani, K. Okumura, Y. Shimabayashi, K. Iwai, *Biosci. Biotechnol. Biochem.* **1992**, *56*, 1921–1923.
[11] A. Kirpal, *Monatsh. Chem.* **1907**, *28*, 439–445.
[12] in *PDF-2*, *Vol.* ICDD, Pennsylvania, USA, **2005**.
[13] F. Takusagawa, K. Hirotsu, A. Shimada, *Bull. Chem. Soc. Jpn.* **1973**, *46*, 2669–2675.
[14] P. J. F. Griffiths, *Acta Crystallogr.* **1963**, *19*, 1074.
[15] K. M. Harmon, K. E. Shaw, *J. Mol. Struct.* **1999**, *513*, 219–230.
[16] P. Vishweshwar, A. Nangia, V. M. Lynch, *J. Org. Chem.* **2002**, *67*, 556–565.
[17] J. Bernstein, R. J. Davey, J.-O. Henck, *Angew. Chem.* **1999**, *111*, 3646–3669; *Angew. Chem. Int. Ed.* **1999**, *38*, 3440–3461.
[18] F. Mongin, F. Trecourt, G. Queguiner, *Tetrahedron Lett.* **1999**, *40*, 5483–5486.
[19] G. H. Suverkropp, P. L. Alsters, C. S. Snijder, J. G. De Vries, (DSM N. V., Neth.), US05917049, **1999**.
[20] H. Briehl, J. Butenuth, *Thermochim. Acta* **1992**, *23*, 121–130.
[21] A monotropic system is defined when only a polymorph is stable at all temperature below the melting point. Although in the case of forms I and II decomposition is observed before melting, the form I seems to be stable at all the temperatures before decomposition, thus it has been defined as a monotropic system.
[22] F. Takusagawa, K. Hirotsu, A. Shimada, *Bull. Chem. Soc. Jpn.* **1973**, *46*, 2372–2380.
[23] F. Takusagawa, K. Hirotsu, A. Shimada, *Bull. Chem. Soc. Jpn.* **1973**, *46*, 2292–2299.
[24] J. A. Cowan, J. A. K. Howard, G. J. McIntyre, S. M. F. Lo, I. D. Williams, *Acta Crystallogr. Sect. B Struct. Sci.* **2005**, *61*, 724–730.
[25] F. H. Allen, O. Kennard, D. G. Watson, L. Brammer, A. G. Orpen, R. Taylor, *J. Chem. Soc. Perkin Trans. 2* **1987**, S1–S19.
[26] G. A. Jeffrey, *An introduction to hydrogen bonding*, Oxford University Press, New York, **1997**.
[27] F. H. Allen, *Acta Crystallogr. Sect. B Struct. Sci.* **2002**, *B58*, 380–388.
[28] L. Wasylina, E. Kucharska, Z. Weglinski, A. Puszko, *Chem. Heterocycl. Compd.* **1999**, *35*, 186–194.
[29] A. Szorcsik, L. Nagy, J. Sletten, G. Szalontai, E. Kamu, T. Fiore, L. Pellerito, E. Kalman, *J. Organomet. Chem.* **2004**, *689*, 1145–1154.
[30] L. Puntus, V. Zolin, V. Kudryashova, *J. Alloys Compd.* **2004**, *374*, 330–334.
[31] C. Qin, X. Wang, E. Wang, L. Xu, *Inorg. Chim. Acta* **2006**, *359*, 417–423.
[32] X. Wang, C. Qin, E. Wang, Y. Li, N. Hao, C. Hu, L. Xu, *Inorg. Chem.* **2004**, *43*, 1850–1856.
[33] V. Zolin, L. Puntus, V. Kudryashova, V. Tsaryuk, J. Legendziewicz, P. Gawryszewska, R. Szostak, *J. Alloys Compd.* **2002**, *341*, 376–380.
[34] A. Novak, *Struct. Bonding (Berlin)* **1974**, *18*, 177–216.
[35] T. L. Threlfall, *Analyst* **1995**, *120*, 2435–2460.
[36] S. Chattopadhyay, S. K. Brahma, *Spectrochim. Acta Part A* **1993**, *49 A*, 589–597.
[37] M. Szafran, Z. Dega-Szafran, G. Buczak, A. Katrusiak, M. J. Potrzebowski, A. Komasa, *J. Mol. Struct.* **1997**, *416*, 145–160.
[38] N. Colthup, L. H. Daly, S. E. Wiberley, *Introduction to Infrared and Raman Spectroscopy*, 2nd ed., **1975**, p. 544.
[39] G. B. Deacon, R. J. Phillips, *Coord. Chem. Rev.* **1980**, *33*, 227–250.
[40] J. Herzfeld, A. E. Berger, *J. Chem. Phys.* **1980**, *73*, 6021–6030.
[41] D. Braga, L. Maini, G. de Sanctis, K. Rubini, F. Grepioni, M. R. Chierotti, R. Gobetto, *Chem. Eur. J.* **2003**, *9*, 5538–5548.
[42] G. C. Levy, R. L. Lichter, *Nitrogen-15 Nuclear Magnetic Resonance Spectroscopy*, **1979**, p. 221.
[43] K. Eichele, R. E. Wasylishen in *HBA ver. 1.5, Program for Herzfeld-Berger analysis, Vol.* Dalhousie University, Halifax, Canada, **2005**.
[44] G. M. Sheldrick, *SHELXL97*, University of Göttingen (Germany), **1997**.
[45] E. Keller, SCHAKAL99, Graphical Representation of Molecular Models, University of Freiburg (Germany), **1999**.

Received: May 31, 2006
Published online: October 31, 2006

